Science of the Total Environment 747 (2020) 141325

Contents lists available at ScienceDirect

Science of the Total Environment

journal homepage: www.elsevier.com/locate/scitotenv

Impacts of the COVID-19 responses on traffic-related air pollution in a Northwestern US city

Jianbang Xiang [a,*], Elena Austin [a], Timothy Gould [b], Timothy Larson [a,b], Jeffry Shirai [a], Yisi Liu [a], Julian Marshall [b], Edmund Seto [a]

[a] Department of Environmental and Occupational Health Sciences, University of Washington, Seattle, WA 98195, United States
[b] Department of Civil and Environmental Engineering, University of Washington, Seattle, WA 98195, United States

HIGHLIGHTS

- The COVID-19 impacts on traffic-related air pollution were evaluated in a US city.
- This study is the first to assess the COVID-19 impacts on roadside UFPs.
- Meteorology was fully adjusted by using multivariate autoregressive models.
- Significant decreases showed in UFPs, black carbon, $PM_{2.5}$, NO, NO_2, NO_x, and CO.

GRAPHICAL ABSTRACT

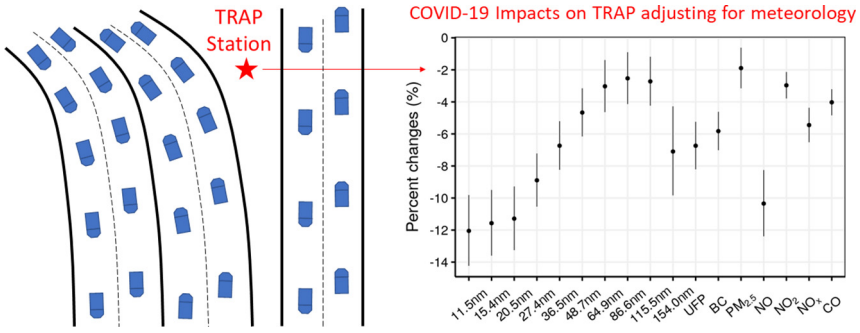

ARTICLE INFO

Article history:
Received 8 June 2020
Received in revised form 19 July 2020
Accepted 27 July 2020
Available online 28 July 2020

Keywords:
COVID-19
Traffic
Air pollution
$PM_{2.5}$
Ultrafine particle (UFP)
Meteorology

ABSTRACT

This study evaluates the COVID-19 impacts on traffic-related air pollution, including ultrafine particles (UFPs), $PM_{2.5}$, black carbon (BC), NO, NO_2, NO_x, and CO in a Northwestern US city. Hourly traffic, air pollutants, and meteorological data on/near a major freeway in the downtown of Seattle, Washington, were collected for five weeks before and ten weeks after the Washington Stay Home Order (SHO) was enacted, respectively (February 17–May 31, 2020). The pollutants between pre- and post-SHO periods were compared, and their differences were statistically tested. Besides, first-order multivariate autoregressive (MAR(1)) models were developed to reveal the impacts specific to the change of traffic due to the COVID-19 responses while controlling for meteorological conditions. Results indicate that compared with those in the post-SHO period, the median traffic volume and road occupancy decreased by 37% and 52%, respectively. As for pollutants, the median BC and $PM_{2.5}$ levels significantly decreased by 25% and 33%, relatively, while NO, NO_2, NO_x, and CO decreased by 33%, 29%, 30%, and 17%, respectively. In contrast, neither size-resolved UFPs nor total UFPs showed significant changes between the two periods, although larger particles (≥115.5 nm) decreased by 4–29%. Additionally, significant differences were found in meteorological conditions between the two periods. Based on the MAR(1) models, controlling for meteorological conditions, the COVID-19 responses were associated with significant decreases in median levels of traffic-related pollutants including 11.5–154.0 nm particles (ranging from −3% [95% confidence interval (CI): −1%, −4%] to −12% [95% CI: −10%, −14%]), total UFPs (−7% [95% CI: −5%, −8%]), BC (−6% [95% CI: −5%, −7%]), $PM_{2.5}$ (−2% [95% CI: −1%, −3%]), NO, NO_2, NO_x (ranging from −3% [95% CI: −2%, −4%] to −10% [95% CI: −18%, −12%]), and CO (−4% [95% CI, −3%, −5%]). These findings illustrate that the conclusion of the COVID-19 impacts on urban traffic-related air pollutant levels could be completely different in scenarios whether

* Corresponding author at: Health Sciences Building, F-224, Seattle, WA 98195, United States.
E-mail address: jx56@uw.edu (J. Xiang).

https://doi.org/10.1016/j.scitotenv.2020.141325

meteorology was adjusted for or not. Fully adjusting for meteorology, this study shows that the COVID-19 responses were associated with much more reductions in traffic-related UFPs than $PM_{2.5}$ in the Seattle region, in contrast to the reverse trend from the direct empirical data comparison.

1. Introduction

The ongoing global pandemic of coronavirus disease (COVID-19) caused by the severe acute respiratory syndrome coronavirus 2 (SARS-CoV-2) has led to more than 355,000 premature deaths worldwide, including 100,000 in the United States (US) alone as of May 27, 2020 (Johns Hopkins University, 2020). Washington State, located in the northwest of the US, first reported a COVID-19 confirmed case on January 20, 2020, and declared a state of emergency on March 3 and issued a Stay Home Order (SHO) on March 23 (see Appendix Fig. A1 for a timeline of events). As a result, the road traffic volume and patterns in Washington were altered. By April 3, traffic on Interstate 5 (I-5) fell by over 50% in both downtown Seattle and Everett (40 km to the north) as compared to typical traffic volumes in February (Washington State Department of Transportation, 2020b). The Stay Home Order, which lasted ten weeks, ended on May 31.

Road traffic is a major urban pollutant source in the Seattle area based on multiple apportionment studies (Friedman, 2020; Larson et al., 2004; Maykut et al., 2003; Wu et al., 2007). Considering the unprecedented decrease of urban traffic due to the COVID-19 responses, a relatively large decrease in urban air pollutant levels was anticipated in Washington and other urban areas around the world. Recent studies conducted in China showed that ambient $PM_{2.5}$, NO_2, SO_2, and CO concentrations during the COVID-19 period decreased by about 30–40%, 30–60%, 20–30%, and 30%, respectively, while O_3 increased about 10%, compared with either the same period in historical years or pre-response period in the same year (Bauwens et al., 2020; Li et al., 2020; Shi and Brasseur, 2020; Xu et al., 2020). Satellite NO_2 data suggested that Western Europe and major Northeastern US cities experienced 20–38% NO_2 decreases in 2020 relative to the same period in 2019 although Iran, a region strongly affected by COVID-19, did not show clear evidence of lower NO_2 concentrations (Bauwens et al., 2020). In the US, preliminary results of an ongoing study utilizing daily $PM_{2.5}$ and O_3 data obtained from US Environmental Protection Agency indicate that $PM_{2.5}$ levels were about 10% higher than expected while O_3 levels were about 7% lower than expected during the post-SHO period compared to the same period in historical years (Bekbulat et al., 2020). Additionally, preliminary analysis of this study shows that NO_2 levels in Seattle were 20% lower than expected (Bekbulat et al., 2020).

The large variation in these findings are explained by the fact that non-COVID-related factors (e.g., meteorology and emissions from regional events other than traffic) may play an important role in confounding these short-term trends (Arya, 1999; Ault et al., 2009; Chen et al., 2017; Husar and Renard, 1998; Statheropoulos et al., 1998; Vu et al., 2015; Zhao et al., 2020). The effects of meteorology and regional events can be partially adjusted by comparing the current year data with historical year data (Bekbulat et al., 2020). Another recent study tried to exclude meteorological impacts on the change of air pollution by using the Weather Research and Forecasting (WRF) model and the Community Multiscale Air Quality (CMAQ) model combining with some attributing analyses (Zhao et al., 2020). However, as stated in the study, WRF and other regional models have difficulties in simulating the evolution of the boundary layer (Banks et al., 2015; Hu et al., 2010), which plays an important role in air pollution formation and dispersion. Therefore, the impacts of meteorological factors may not be completely and accurately captured by the WRF model. Hence, it is of great value to develop an approach to account for these confounding factors fully. Road traffic emits a wide variety of pollutants and is one of the main contributors of urban ultrafine particles (UFPs; diameter ≤ 100 nm) (Harrison et al., 2011; Pant and Harrison, 2013; Vu et al., 2015) and black carbon (BC) (Miguel et al., 1998; Zheng et al., 2015), no studies have examined the COVID-19 impacts on ambient UFPs and only one study in Milan, Italy involved BC (Collivignarelli et al., 2020), to the authors' knowledge.

Near-roadside sampling was conducted in Seattle, Washington, preceding and following the Washington State SHO. Pollutant data collected at a roadside monitoring station in Seattle was combined with roadway traffic and meteorology data to better understand any changes in air quality related to decreased traffic. This paper aims to evaluate the impacts of the COVID-19 responses on traffic and corresponding traffic-related air pollution (TRAP), including UFPs, $PM_{2.5}$, BC, NO, NO_2, NO_x, and CO. In particular, this paper examined the impacts by (1) comparing the pollutants between pre- and post-SHO periods based on the empirical data, and (2) developing a model that controlled for meteorological conditions to reveal the impacts specific to the change of traffic due to the COVID-19 responses.

2. Methods

2.1. Data sources

The Washington State Department of Transportation (WSDOT) operates multiple loop detector stations along main routes in Washington, including I-5, which connects Canada, Washington, Oregon, California, and Mexico from north to south. The hourly traffic data from February 17 to May 31, 2020, at I-5 milepost 164.66 (close to 10th Ave S & S Weller St, Seattle, see Appendix Fig. A2 for the location) were obtained from the TRACFLOW system maintained by WSDOT (Washington State Department of Transportation, 2020a). Parameters used in this study include hourly total vehicle (TOV) volume summing all mainline lanes in both directions and road occupancy (%) defined as a percent of the time a short space on the road is occupied by vehicles (Hall, 1996). Traffic data were excluded as invalid or unusable under one or more of the following conditions: (1) flagged as errors by the TRACFLOW system; (2) volume or occupancy was less than 0; (3) time when the loop detectors were working in only one direction (either northbound or southbound).

Pollutants were monitored at a roadside air quality monitoring station (Seattle-10th & Weller), approximately 10 m east of the loop detectors on I-5 (see Appendix Fig. A2 for the location). Hourly BC and $PM_{2.5}$ mass concentrations, as well as NO, NO_2, NO_x, and CO volume concentrations from February 17 to May 31, 2020, at this site, were obtained from the Washington Air Quality Advisory (WAQA) system maintained by the Washington State Department of Ecology (WSDOE) (Washington State Department of Ecology, 2020). Size-resolved nanoparticles were measured at 1-minute intervals from March 7 to May 31, 2020, using a NanoScan SMPS Nanoparticle Sizer (Model 3910, TSI Inc., MN) deployed at the same site by our team from University of Washington. The NanoScan measures particle number concentrations (PNCs) over a size range of 10 to 420 nm particles with a resolution of 13 size bins (11.5 nm, 15.4 nm, 20.5 nm, 27.4 nm, 36.5 nm, 48.7 nm, 64.9 nm, 86.6 nm, 115.5 nm, 154.0 nm, 205.4 nm, 273.8 nm, 365.2 nm). Pollutant data were excluded under one or more of the following conditions: (1) flagged as errors by the WAQA system or the NanoScan instrument; (2) pollutant level was less than 0; (3) incomplete hourly measures by the NanoScan (< 50% minute data). We

additionally limited the size-resolved data from the NanoScan to the size bins <205.4 nm as the larger bins reported more than 50% of zeros.

Hourly meteorological data, including ambient wind direction and speed, as well as the temperature at the Seattle-10th &Weller monitoring station, were obtained from the WAQA system. Hourly ambient relative humidity (RH) and precipitations were obtained from the BFI station (about 7.5 km south of the Seattle-10th & Weller site) in Washington State Automated Surface Observing System (ASOS) Network (Iowa Environmental Mesonet, 2020) as they were not routinely monitored at the Seattle-10th & Weller site.

2.2. Empirical data comparisons between pre- and post-SHO periods

Considering the weekly pattern of traffic, the data from February 17 to May 31, 2020, were grouped into fifteen weeks, including the pre-SHO period (five weeks, February 17–March 22, 2020) and the post-SHO period (ten weeks, March 23–May 31, 2020). The week right before the Washington SHO enacted was defined as Week 0 (March 16–22, 2020). Note that size-resolved PNC data measured from NanoScan were not available for Weeks (−4) to (−3), while all other traffic, pollutant, and meteorological data were available for the entire fifteen-week period.

Total UFP number concentrations (NCs) were calculated by summing the PNCs of eight size bins (median sizes ranging from 11.5–86.6 nm). The PNC data were aggregated into hourly means after applying the aforementioned exclusion criteria. Then, the fifteen-week traffic, pollutant, and meteorological data were merged based on date and hourly time.

None of the traffic, pollutant, and meteorological variables were normally distributed based on Shapiro-Wilk tests. Therefore, Wilcoxon two-sample rank-sum tests were conducted for each traffic, pollutant, and meteorological variable between the pre- and post-SHO periods to compare the differences between these two periods. Wilcoxon effect sizes, which indicate the strength of the differences were calculated using the "coin" and "rstatix" packages in R (R Core Team, 2013).

2.3. Model prediction of COVID-19 impacts on TRAP

Road occupancy is an equivalent variable to traffic density, which can be expressed as traffic volume divided by speed (Hall, 1996). Theoretically, TRAP levels at a near-road monitoring site should be directly related to the traffic density rather than volume, although traffic density and volume are highly correlated. Additionally, road occupancy in the adjacent areas between the west and east of the air monitoring station should be much more similar than traffic volume. Therefore, the change of road occupancy was used as the primary indicator for TRAP impacts due to the COVID-19 responses in the present study.

Due to the potential autocorrelation among observations from the time-series air pollution measurement, multivariate autoregressive (MAR) models were used to analyze traffic-pollutant associations between road occupancy and each pollutant level (Holmes et al., 2020; Neumaier and Schneider, 2001). Based on the partial autocorrelation function (PACF) computing for each pollutant, the p orders for the MAR(p) models were set to 1 for all pollutants (Fig. A3), which means the pollutant at time t was based on the immediately preceding value at time t-1. Depending on data distribution and statistical tests, pollutant concentrations were natural log-transformed in the MAR(1) models. With road occupancy as the main traffic-related indicator, the models (Eq. (1)) were fitted for each pollutant in which the dependent variable was the natural log-transformed pollutant level at time t ($\log(y_t)$), and the independent variables included the natural log-transformed pollutant level at lag hour 1 ($\log(y_{t-1})$), traffic-related indicator ($traffic_t$), and meteorological variables such as temperature (T_t), relative humidity (RH_t), precipitation (P_t), wind speed (WS_t), and a category variable – wind direction (WD_t). According to the layout of I-5 near the air quality monitoring station (Fig. A2), wind direction (degrees from the north) was categorized based on a northwest-southeast line (i.e., 135–315 degrees as the reference category (level = 0, mostly west wind), and the rest as the other category (level = 1, mostly east wind)). Outliers were determined by using Cook's distance value. The observations with Cook's distance value greater than 0.5 were excluded from the regression analysis (Cook, 1977; Yerramshetty and Akkus, 2008).

$$\log(y_t) = \beta_0 + \beta_1 \log(y_{t-1}) + \beta_2 traffic_t + \beta_3 T_t + \beta_4 RH_t + \beta_5 P_t + \beta_6 WS_t + \beta_7 WD_t + \varepsilon \quad (1)$$

where β_0 – β_7 are the coefficients from the MAR(1) model; ε is the residual.

The estimates of β_2 determined from the MAR(1) models were used to predict the median percent changes of pollutant levels due to the COVID-19 responses, as shown in Eq. (2):

$$\Delta y(\%) = \left(e^{\beta_2 \times \Delta_{traffic}} - 1\right) \times 100\% \quad (2)$$

where $\Delta_{traffic}$ is the median absolute change of road occupancy due to the COVID-19 responses.

Based on pairwise comparisons using Wilcoxon rank-sum tests, the median road occupancy was not statistically different ($p > 0.2$) among Weeks (−4), (−3), and (−2), but statistically different ($p < 0.05$) between Week (−2) and Week (−1) (see more in the Results section). As there were no significant differences for the median hourly traffic between Week (−2) and previous weeks, and all data were available in Week (−2), Week (−2) was taken as the reference week when there were no significant impacts on the median traffic from the COVID-19 responses. Therefore, $\Delta_{traffic}$ was calculated as the difference of median hourly traffic between the post-SHO weeks and Week (−2), as shown in Eq. (3):

$$\Delta traffic = traffic_{post-SHO} - traffic_{Week(-2)} \quad (3)$$

where $traffic_{post\text{-}SHO}$ and $traffic_{Week(-2)}$ are the median hourly road occupancy during Weeks 1 to 10 and Week (−2), respectively.

The median absolute changes of pollutant levels due to the COVID-19 responses were calculated by multiplying the percent changes with the median hourly concentration in Week (−2) for each pollutant, respectively.

2.4. Sensitivity analyses

In the main model, data in Week 0 were excluded as there probably existed significant air pollution emission sources from regional events in that week (see more in the Results section). The sensitivity of the MAR(1) results to the data in Week 0 was examined by including the data in Week 0. Additionally, based on the wind rose plot (Appendix Fig. A4), the sensitivity to the wind direction categorizing was examined by categorizing the wind direction based on a north-south line into the west (180–360 degrees, reference category) and the east (0–180 degrees). Also, five more models were assessed: (1) without considering the autocorrelation effects in the time-series observations (excluding the $\log(y_{t-1})$ variable in the MAR(1) model), (2) with a second-order multivariate autoregressive (MAR(2)) model, (3) considering the interaction between the amount of road occupancy and the two WD categories, (4) using traffic TOV volume as the main traffic indicator instead of road occupancy, and (5) using last-hour road occupancy as the main lag-effect indicator instead of last-hour pollutant level. The results were compared with those of the main models.

For all statistical tests, $p = 0.05$ indicated statistical significance in this study. All calculations and figures were made using "data.table", "stats", "mgcv", "coin" and "rstatix", "tidyverse", "openair","ggplot2", "ggpubr" and "leaflet" packages in R, Version 3.3.0 embedded in RStudio Version 1.1.456.

3. Results

3.1. Weekly variation

Fig. 1 shows the weekly traffic (volume and occupancy), pollutant concentrations (size-resolved particles and total UFPs, BC, $PM_{2.5}$, NO, NO_2, NO_x, and CO), and meteorological conditions (wind direction, wind speed, temperature, relative humidity, and precipitation) at Seattle 10th & Weller for both pre-SHO (Weeks (−4) to 0) and post-SHO (Weeks 1 to 10) periods. The traffic TOV volume and road occupancy continually decreased from Weeks (−3) to 1 by ~50% for medians, including a decrease of ~30% for medians from Weeks 0 to 1. This suggests that the COVID-19 pandemic impacts on traffic in Seattle were observed from early March (Week (−2)), and the SHO enacted on March 23 (the first day of Week 1) resulted in an additional reduction in the traffic volume and road occupancy. This is consistent with the timeline of major governmental and public responses in Washington, as shown in Appendix Fig. A1. While significantly lower than that in the pre-SHO period, the traffic from Weeks 1 to 10 in the post-SHO period gradually increased. By the end of the post-SHO period (Week 10), the median traffic TOV volume and road occupancy were 68% and 54% of those in Week (−2), respectively.

The concentrations of BC, $PM_{2.5}$, and gaseous pollutants seem to be generally higher in the pre-SHO period than those in the post-SHO period, while the trend is unclear for UFPs. It can be clearly seen that the trend of weekly variation of all pollutants does not mirror that of traffic, especially for Week 0, where an unexpected spike in most pollutants is observed. Relatively large drops in concentrations were observed in most pollutants, except in 11.5–20.5 nm particles, from Weeks 0 to 1. For instance, median UFPs, $PM_{2.5}$, and NO_x concentrations decreased by 43%, 75%, and 52%, respectively. The lower wind speed in Week 0 relative to that in Weeks (−1) and 1 possibly contributed to the spike in that week. However, this cannot explain why BC, $PM_{2.5}$, NO_2, and NO_x levels in Week 0 were significantly higher than those in Week (−3) even though wind speed and other meteorological variables were comparable in the two weeks, while traffic volume and road occupancy in Week 0 decreased by 25% and 53% relative to those in Week (−3), respectively. It can be inferred that there probably existed significant air pollution emission sources from regional events in Week 0.

3.2. Empirical data comparisons between pre- and post-SHO periods

As regional events showed a large impact on pollutants at Seattle-10th &Weller monitoring station in Week 0, the effects of SHO enactment could have been overestimated with this outlier. Therefore, excluding the data in Week 0, Fig. 2 shows the pooled density distributions of traffic, pollutant concentrations, and meteorological conditions at Seattle 10th & Weller for both the pre- and post-SHO periods. Appendix Table A1 summarizes the statistic descriptions of traffic, pollutant levels, and meteorological conditions for each period as well as comparisons between the two periods, excluding the data in Week 0. Compared with those in the post-SHO period, the median traffic volume and road occupancy decreased from 6656 to 4181 #/h (a drop of ~37%), and from 23% to 11% (a drop of ~52%), respectively. As for pollutants, the median BC and $PM_{2.5}$ levels decreased by 25% and 33%, relatively, while NO, NO_2, NO_x, and CO decreased by 33%, 29%, 30%, and 17%, respectively. In contrast, although larger particles (≥115.5 nm) decreased by 4–29%, neither size-resolved UFPs nor total UFPs show significant changes between the two periods. As for meteorological conditions, there was more wind from the west (degree >180) in the post-SHO period. Compared with those in the pre-SHO period, median wind speed and temperature increased by 0.3 m/s (19%) and 6 °C, respectively, while relative humidity decreased by 7%. Median precipitations were both 0 μm in the two periods, while mean precipitation increased by 21 μm (122%) in the post-SHO period. Wilcoxon tests indicate that the differences between pre- and post-SHO periods are significant for all traffic, pollutants except 11.5–115.5 nm particles, and meteorology variables except precipitation. Additionally, the tests show moderate effects ($0.3 \le r < 0.5$) for traffic volume, road occupancy, NO_2, CO, and temperature, and small effects ($r < 0.3$) for the other variables.

Appendix Table A2 summarizes the statistic descriptions of traffic, pollutant levels, and meteorological conditions for each period as well as comparisons between the two periods, including the data in Week 0. Including the data in Week 0 would make the two-period differences significant for larger UFPs (≥36.5 nm) and increase the effect size for almost all pollutants.

3.3. Model prediction

Appendix Table A3 summarizes the results of the main MAR (1) models. The regression coefficients of traffic indicators (β_2) are significant for all pollutants ($p < 0.005$). The coefficient of determination (R^2) for all the models ranges from 0.5 to 0.8, which generally indicates 50–80% of data variances can be explained by the main MAR(1) models. In addition, Appendix Fig. A5 shows the results of the autocorrelation function (ACF) computing of the residuals for each pollutant in the main MAR(1) models. Results indicate no autocorrelation in the residuals for each pollutant, confirming that the MAR(1) models well captured the autocorrelation effects in the time-series observations of pollutants.

Compared with the reference week in the pre-SHO period, the median road occupancy in the post-SHO period decreased by 53%. Fig. 3 shows the MAR(1) results for the effect of COVID-19 pandemic response on air pollutants fully adjusted for meteorological conditions. All pollutant variables were significantly lower in the post SHO period. In particular, there were significant decreases in median levels of 11.5–154.0 nm particles (ranging from −3% [95% CI: −1%, −4%] to −12% [95% CI: −10%, −14%]), total UFPs (−7% [95% CI: −5%, −8%]), BC (−6% [95% CI: −5%, −7%]), $PM_{2.5}$ (−2% [95% CI: −1%, −3%]), NO, NO_2, NO_x (ranging from −3% [95% CI: −2%, −4%] to −10% [95% CI: −18%, −12%]), and CO (−4% [95% CI: −3%, −5%]). Nucleation-mode particles (<30 nm) and NO show the largest median percent changes (~10%), followed by 36.5–154.0 nm particles, BC, NO_2, NO_x, and CO. $PM_{2.5}$ shows the smallest percent change which is about 1/3 of that in total UFPs. The corresponding median absolute changes in those pollutants are shown in Appendix Fig. A6. The reductions in median PNCs were generally lower than 150 #/cm^3 for size-resolved particles and ~600 #/cm^3 for total UFPs. In contrast, the reductions in $PM_{2.5}$ and BC mass concentrations were relatively small (<0.1 μg/m^3). Those in NO_x and CO were 2 and 15 ppb, respectively.

3.4. Sensitivity analyses

The results of the sensitivity analyses are shown in Appendix Figs. A7–12, and Table A4. Including the data in Week 0 (Fig. A7) or categorizing the wind direction in the other way (Fig. A8) slightly changed the results (changes ranging from −1 to 1% compared with the main models). Ignoring the autocorrelation effects in the time-series observations resulted in much larger reductions in all pollutants (changes ranging from 3 to 22%), especially for nucleation-mode particles (<30 nm), BC, and NO (Fig. A9). However, the R^2 of this model (0.1–0.5) is much smaller, and the Akaike and Bayes information criteria are much larger, compared with the main models (Table A4). The MAR(2) model made slight differences to the results (changes ranging from 0 to 1%), further confirming that the MAR(1) models are good enough to capture the autocorrelation effects (Fig. A10). Including an interaction between the amount of road occupancy and the two WD categories did not improve the model, and the coefficients for the interaction term are nonsignificant for nearly half of the pollutants. It can be inferred that road occupancy on I-5 well represented the road occupancy in both west and east of the air monitoring station. Using traffic TOV volume as the main indicator instead of road occupancy resulted in larger reductions

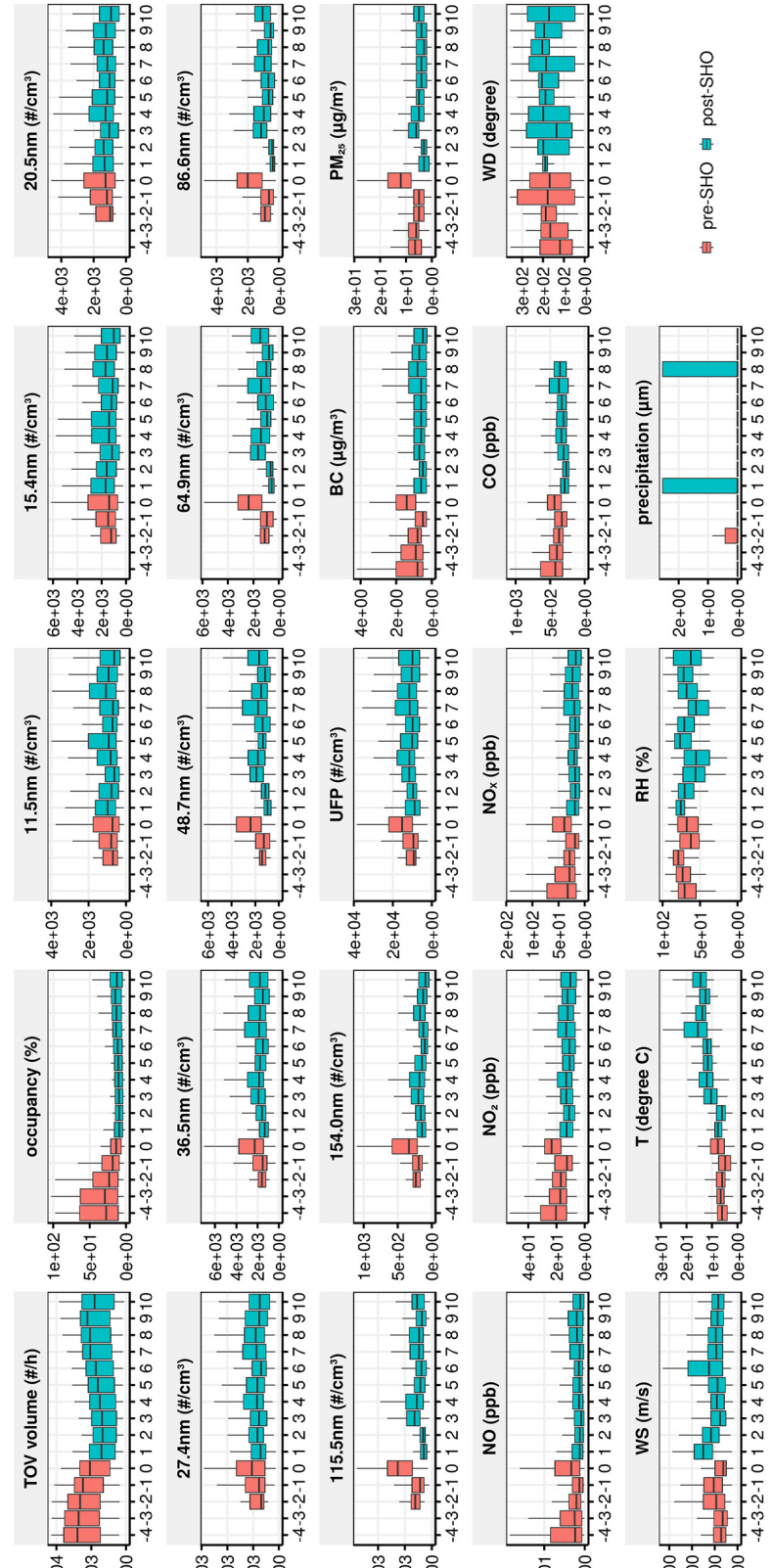

Fig. 1. Weekly boxplots of traffic, air pollutants, and meteorological data from the Seattle-10th & Weller monitoring site in the pre- and post-SHO periods. Week 1 was March 23–29, 2020. The size-resolved particles were not available in Weeks (−4) and (−3). All other pollutants and meteorology parameters were measured by government facilities continuously. Outliners (larger than Q3 + 1.5*IQR or smaller than Q1 − 1.5*IQR) were excluded from the figure. *Definition of abbreviations:* TOV = total vehicle; 11.5 nm–154.0 nm = 11.5 nm–154.0 nm particles; PNC = particle number concentration; BC = black carbon; WD = wind direction (degrees from the north); WS = wind speed; T = temperature; RH = relative humidity; SHO = Stay Home Order; Q1 = 25th quantile; Q3 = 75th quantile; IQR = interquartile range.

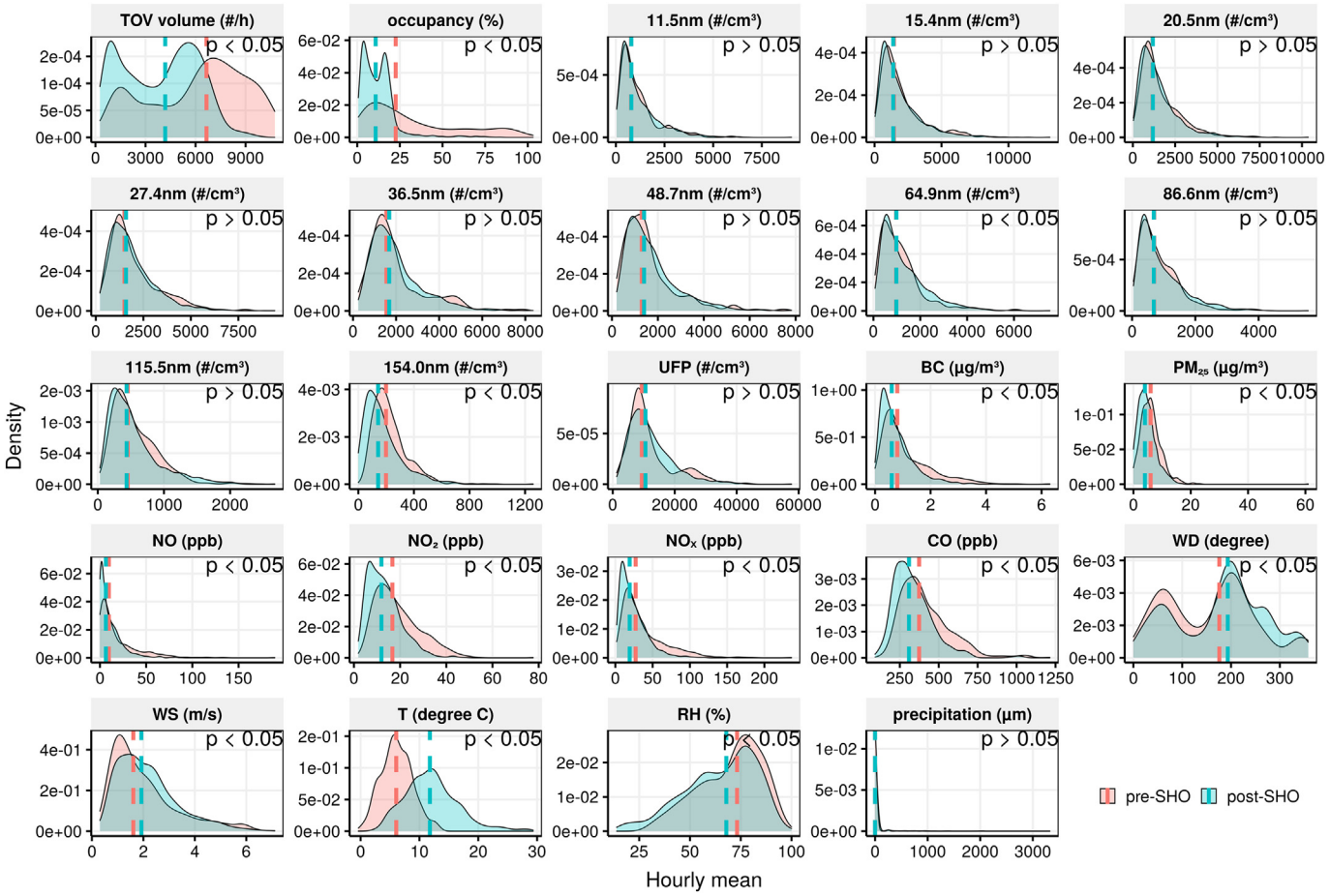

Fig. 2. Pooled density plot of traffic, pollutant, and meteorological data from the Seattle-10th & Weller monitoring site in the pre- and post-SHO periods. The colored dashed line on each panel represents the median for the corresponding distribution. P-value is shown at the top right corner of each panel. *Definition of abbreviations*: TOV = total vehicle; 11.5 nm–154.0 nm = 11.5 nm–154.0 nm particles; PNC = particle number concentration; BC = black carbon; WD = wind direction (degrees from the north); WS = wind speed; T = temperature; RH = relative humidity; SHO = Stay Home Order.

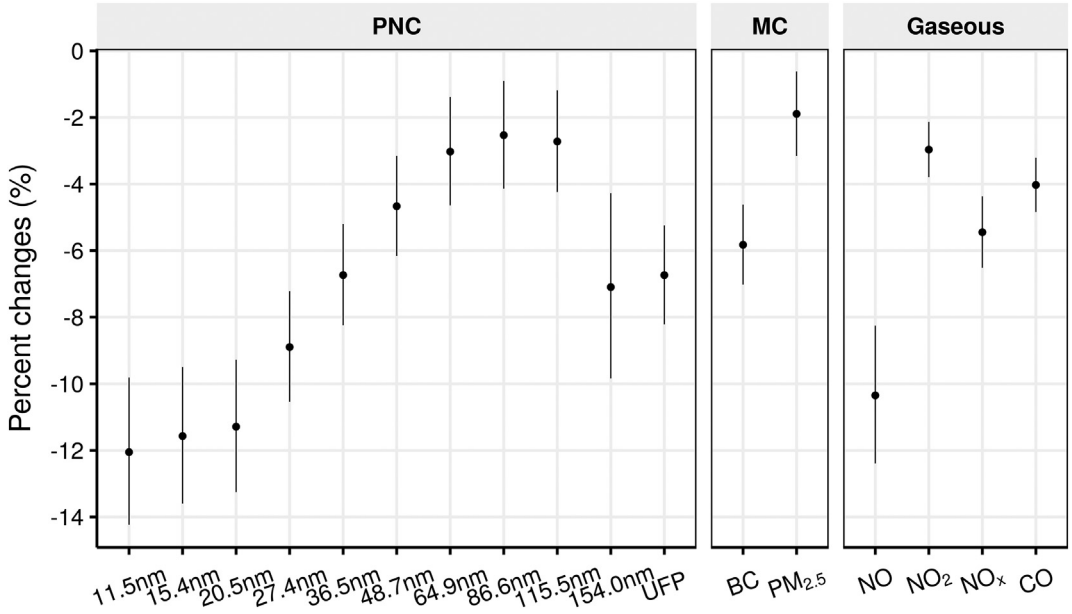

Fig. 3. Mean with 95% confidence interval of median percent changes in near-road air pollutants associated with the COVID-19 responses in fully adjusted first-order multivariate autoregressive (MAR(1)) models. *Definition of abbreviations*: 11.5 nm – 154.0 nm = 11.5 nm – 154.0 nm particles; PNC = particle number concentration; MC = mass concentration; BC = black carbon.

in all pollutants except 115.5 nm particles and $PM_{2.5}$, although the result for $PM_{2.5}$ became statistically nonsignificant ($p = 0.1$) (Fig. A11). Additionally, using last-hour road occupancy as the main lag-effect indicator instead of last-hour pollutant level resulted in much larger reductions in most pollutants, despite that the results are nonsignificant for 64.9–86.6 nm particles and $PM_{2.5}$ (Fig. A12). However, the R^2 of this model (0.1–0.5) is much smaller, and the Akaike and Bayes information criteria are much larger, compared with the main models (Table A4).

Despite the variations in pollutant percent change predictions among all the models, the relative magnitudes among different pollutants are generally unchanged. It further indicates traffic contributed more to UFPs, BC, and NO, than $PM_{2.5}$ and CO. The main models generally have the larger R^2 and smaller Akaike and Bayes information criteria compared with the sensitivity analysis models, and the results from the main models are statistically significant. Therefore, the results from the main model analyses are primarily reported.

4. Discussion

Previous studies have examined the impacts of the COVID-19 responses on ambient $PM_{2.5}$ and/or some other gaseous pollutants in China (Bauwens et al., 2020; Chen et al., 2020; Li et al., 2020; Shi and Brasseur, 2020; Xu et al., 2020), India (Sharma et al., 2020), Italy (Collivignarelli et al., 2020), Brazil (Nakada and Urban, 2020), and NO_2 in Western Europe and major Northeastern US cities (Bauwens et al., 2020). Additionally, an ongoing study has estimated the impacts on $PM_{2.5}$ and O_3 across the US, as well as NO_2 in three US cities, including Seattle (Bekbulat et al., 2020). Another recent study tried to exclude meteorological impacts on the change of air pollution during the COVID outbreak by using the WRF model (Zhao et al., 2020). However, the impacts of meteorological factors may not be completely and accurately excluded due to the inherent limitations of the WRF model (Zhao et al., 2020). To the authors' knowledge, the present study is the first to examine the impacts of the COVID-19 responses on size-resolved and total UFPs, and the first to reveal the impacts on TRAP specific to the change of traffic after fully adjusting for meteorological variations.

In the main analyses, the model predictions were based on the median reduction of road occupancy between the pre- and post-SHO periods. Although the mean hourly road occupancy in Week (−2) was ~10% lower than that in Week (−3), the medians showed no statistically significant differences ($p > 0.2$) due to the right-skewed distribution of road occupancy. Thus, Week (−2) was utilized as the pre-SHO reference week. It makes no statistically significant differences for the predicted percent reductions in all pollutants to take Week (−3) as the reference. However, based on Wilcoxon two-sample rank-sum tests, there were significant decreases for median $PM_{2.5}$ and CO concentrations from Weeks (−3) to (−2) ($p < 0.05$), although the effect sizes were small ($r < 0.3$). This indicates that traffic was not the only contributor to these pollutants. In addition to meteorological conditions, there were probably other contributors since $PM_{2.5}$ and CO are both commonly from anthropogenic and natural sources (Hudman et al., 2008; Larson et al., 2004). Both percent and absolute changes associated with the impacts of the COVID-19 responses should be interpreted with caution. They represented the magnitude of the impacts when traffic changed while other factors (e.g., meteorology) remain constant.

The autocorrelation effects in the time-series observations of pollutants played an important role in the MAR(1) models. In this study, 50–80% of the pollutant concentrations at the last hour contributed to the pollutant levels at the current hour. Thus, without considering the autocorrelation would generally result in the worse fitting. On the other hand, the autocorrelation effects indicate that the current-hour traffic had impacts on both current- and next-hour pollutant levels at the monitoring station. The current MAR(1) models, primarily predicting the air pollution impacts based on the current-hour traffic, tend to underestimate the impacts of traffic. However, models including a last-hour road occupancy variable in the model result in much worse fitting and larger uncertainties, as shown in the Sensitivity Analyses. Thus, the results from the main MAR(1) models were reported as the main results.

Meteorology conditions have large impacts on TRAP levels. Based on the results seen in this study, TRAP levels were generally negatively associated with wind speed, precipitations, RH, and temperature, despite the varying magnitudes for different pollutants. Compared with the "west" wind (135–315 degrees), the "east" wind (0–135 and 315–360 degrees) generally led to lower TRAP levels, reflecting that the air pollution level was generally lower in the east of the monitoring site. Compared with those in the pre-SHO period, temperature and wind speed significantly increased while RH significantly decreased in the post-SHO period. Also, there was significantly more wind from the west in which the pollutant levels were generally higher. Without adjusting the meteorology variables, it would be challenging to examine the impacts of COVID-19 responses on TRAP levels. In particular, the impacts on UFPs would be greatly underestimated while impacts on $PM_{2.5}$, BC, NO_x, and CO would be greatly overestimated based on a direct comparison of the empirical data between the pre- and post-SHO periods (Fig. A13). Comparing the post-responses periods with either the same period in historical years or the pre-response period in the same year cannot fully account for the variation of meteorology, which prevents us from observing the effects of the COVID-19 responses. The MAR(1) models developed in this study provide a way to estimate the impacts on traffic-specific air pollutants after excluding major confounding factors.

Based on the empirical data, the median NO_2 levels in the post-SHO period decreased by 29% compared with those in the pre-SHO period. This reduction is comparable to that in another study (Bekbulat et al., 2020), which reported a 20% reduction of NO_2 in Seattle. However, the magnitudes of the reductions in $PM_{2.5}$, NO_2, and CO after adjusting for regional events and meteorological variation in this study are much smaller than those reported in other countries (Bauwens et al., 2020; Li et al., 2020; Shi and Brasseur, 2020; Xu et al., 2020) and in other parts of the US (Bauwens et al., 2020; Bekbulat et al., 2020). This can be explained by five reasons: (1) the results herein are specific to the change in traffic while the other studies included the changes in all anthropogenic sources; (2) the results herein were fully adjusted for meteorology while those in the other studies were not; (3) the contributions of traffic to different air pollutants tend to vary spatially and temporally; (4) the MAR(1) models used in the present study tend to underestimate the impacts of current-hour traffic on next-hour air pollution, as discussed above; and (5) the results in the present study are based on medians while those in some previous studies were based on means (Bauwens et al., 2020; Li et al., 2020). Due to the right-skewed distributions of air pollutant levels, the mean reductions were generally larger than median reductions. With the mean reduction of road occupancy as the prediction metric, the predicted percent reductions in pollutants would be 1–7% larger compared with the main model (Fig. A14). This study reveals that traffic was generally not a major contributor to ambient $PM_{2.5}$ in the Seattle downtown area. This is consistent with the Washington State 2014 Comprehensive Emissions Inventory in which they reported that 2% of annual statewide $PM_{2.5}$ emissions were from on-road mobile sources (Washington State Department of Ecology, 2018). In contrast, traffic was a relatively larger contributor to roadside UFPs, especially nucleation-mode particles (<30 nm).

This study has several limitations. *First*, UFPs were not measured during Weeks (−4) and (−3) in the pre-SHO period, which may lead to biased results compared with BC, $PM_{2.5}$, and gaseous pollutants. However, the MAR(1) models based on hourly data can mostly eliminate the bias because the diurnal variations of traffic provided a wide range to the inputs of the models. *Second*, due to data constraints, the variation of air pollution sources other than traffic emission was not included in the MAR(1) models. Nonetheless, it is reassuring that the results here remained robust in the sensitivity analyses, including the

data in Week 0, when air pollutants at Seattle-10th & Weller were significantly elevated by the air pollution emission sources from regional events. *Finally*, the quantitative results obtained in this study are specific to the Seattle area, where the study was conducted. More studies are warranted to examine whether the results derived from this study are representative of other locations in the US.

5. Conclusions

This study illustrates that the conclusion of the COVID-19 impacts on urban traffic-related air pollutant levels could be completely different in scenarios whether meteorology was adjusted for or not. Fully adjusting for meteorology, this study shows that the COVID-19 responses were associated with much more reductions in traffic-related UFPs than $PM_{2.5}$ in the Seattle region, in contrast to the reverse trend from the direct empirical data comparison. These findings suggest the need for fully adjusting for meteorology in future studies examining the impacts of social/economic interventions on air pollution.

CRediT authorship contribution statement

Jianbang Xiang: Conceptualization, Methodology, Software, Data curation, Formal analysis, Supervision, Writing - original draft, Writing - review & editing. **Elena Austin:** Conceptualization, Methodology, Writing - review & editing. **Timothy Gould:** Data curation, Writing - review & editing. **Timothy Larson:** Conceptualization, Methodology, Writing - review & editing. **Jeffry Shirai:** Writing - review & editing. **Yisi Liu:** Writing - review & editing. **Julian Marshall:** Writing - review & editing. **Edmund Seto:** Conceptualization, Methodology, Supervision, Writing - review & editing.

Declaration of competing interest

The authors declare that they have no known competing financial interests or personal relationships that could have appeared to influence the work reported in this paper.

Acknowledgments

The authors wish to express special thanks to Mr. Manouchehr Goudarzi and Dr. Hui Dong from Washington State Department of Transportation (WSDOT) for helping the authors understand the traffic data, as well as Washington State Department of Transportation Washington State Department of Ecology's (WSDOE) Air Quality Program and Northwest Regional Office for providing access to Seattle-10th & Weller air pollution monitoring site for measurement and data collection.

Funding sources

The study was funded by the City of Seattle for the Beacon Hill Noise Study and Award Number 5R33ES024715-05 from the National Institute of Environmental Health Sciences.

Appendix A. Supplementary data

Supplementary data to this article can be found online at https://doi.org/10.1016/j.scitotenv.2020.141325.

References

Arya, S.P., 1999. Air Pollution Meteorology and Dispersion. vol 6. Oxford University Press, New York.

Ault, A.P., Moore, M.J., Furutani, H., Prather, K.A., 2009. Impact of emissions from the Los Angeles port region on San Diego air quality during regional transport events. Environ. Sci. Technol. 43, 3500–3506.

Banks, R.F., Tiana-Alsina, J., Rocadenbosch, F., Baldasano, J.M., 2015. Performance evaluation of the boundary-layer height from lidar and the Weather Research and Forecasting model at an urban coastal site in the north-east Iberian Peninsula. Bound.-Layer Meteorol. 157, 265–292.

Bauwens, M., Compernolle, S., Stavrakou, T., Müller, J.F., van Gent, J., Eskes, H., et al., 2020. Impact of coronavirus outbreak on NO2 pollution assessed using TROPOMI and OMI observations. Geophys. Res. Lett. 47, e2020GL087978.

Bekbulat, B., Apte, J.S., Millet, D.B., Robinson, A., Wells, K.C., Marshall, J.D., 2020. PM2.5 and ozone air pollution levels have not dropped consistently across the US following societal COVID response. ChemRxiv Preprint https://chemrxiv.org/articles/PM2_5_and_Ozone_Air_Pollution_Levels_Have_Not_Dropped_Consistently_Across_the_US_Following_Societal_Covid_Response/12275603.

Chen, D., Liu, X., Lang, J., Zhou, Y., Wei, L., Wang, X., et al., 2017. Estimating the contribution of regional transport to PM2.5 air pollution in a rural area on the North China Plain. Sci. Total Environ. 583, 280–291.

Chen, K., Wang, M., Huang, C., Kinney, P.L., Anastas, P.T., 2020. Air pollution reduction and mortality benefit during the COVID-19 outbreak in China. Lancet Planet. Health 4, e210–e212.

Collivignarelli, M.C., Abbà, A., Bertanza, G., Pedrazzani, R., Ricciardi, P., Carnevale Miino, M., 2020. Lockdown for CoViD-2019 in Milan: what are the effects on air quality? Sci. Total Environ. 732, 139280.

Cook, R.D., 1977. Detection of influential observation in linear regression. Technometrics 19, 15–18.

Friedman, B., 2020. Source apportionment of PM2.5 at two Seattle chemical speciation sites. J. Air Waste Manage. Assoc. 70, 687–699.

Hall, F.L., 1996. Traffic stream characteristics. Traffic Flow Theory. US Federal Highway Administration, p. 36.

Harrison, R.M., Beddows, D.C., Dall'Osto, M., 2011. PMF analysis of wide-range particle size spectra collected on a major highway. Environ. Sci. Technol. 45, 5522–5528.

Holmes, E.E., Scheuerell, M.D., Ward, E.J., 2020. Applied Time Series Analysis for Fisheries and Environmental Data. NOAA Fisheries, Northwest Fisheries Science Center, Seattle, WA.

Hu, X.-M., Nielsen-Gammon, J.W., Zhang, F., 2010. Evaluation of three planetary boundary layer schemes in the WRF model. J. Appl. Meteorol. Climatol. 49, 1831–1844.

Hudman, R.C., Murray, L.T., Jacob, D.J., Millet, D.B., Turquety, S., Wu, S., et al., 2008. Biogenic versus anthropogenic sources of CO in the United States. Geophys. Res. Lett. 35.

Husar, R.B., Renard, W.P., 1998. Ozone as a Function of Local Wind Speed and Direction: Evidence of Local and Regional Transport. Air and Waste Management Association, Pittsburgh, PA (United States).

Iowa Environmental Mesonet, 2020. ASOS network. URL. https://mesonet.agron.iastate.edu/request/download.phtml?network=WA_ASOS. (Accessed 20 May 2020).

Johns Hopkins University, 2020. COVID-19 dashboard. URL. https://coronavirus.jhu.edu/map.html. (Accessed 24 May 2020).

Larson, T., Gould, T., Simpson, C., Liu, L.-J.S., Claiborn, C., Lewtas, J., 2004. Source apportionment of indoor, outdoor, and personal PM2.5 in Seattle, Washington, using positive matrix factorization. J. Air Waste Manage. Assoc. 54, 1175–1187.

Li, L., Li, Q., Huang, L., Wang, Q., Zhu, A., Xu, J., et al., 2020. Air quality changes during the COVID-19 lockdown over the Yangtze River Delta Region: an insight into the impact of human activity pattern changes on air pollution variation. Sci. Total Environ. 732, 139282.

Maykut, N.N., Lewtas, J., Kim, E., Larson, T.V., 2003. Source apportionment of PM2.5 at an urban IMPROVE site in Seattle, Washington. Environ. Sci. Technol. 37, 5135–5142.

Miguel, A.H., Kirchstetter, T.W., Harley, R.A., Hering, S.V., 1998. On-road emissions of particulate polycyclic aromatic hydrocarbons and black carbon from gasoline and diesel vehicles. Environ. Sci. Technol. 32, 450–455.

Nakada, L.Y.K., Urban, R.C., 2020. COVID-19 pandemic: impacts on the air quality during the partial lockdown in São Paulo state, Brazil. Sci. Total Environ. 730, 139087.

Neumaier, A., Schneider, T., 2001. Estimation of parameters and eigenmodes of multivariate autoregressive models. ACM Trans. Math. Software (TOMS) 27, 27–57.

Pant, P., Harrison, R.M., 2013. Estimation of the contribution of road traffic emissions to particulate matter concentrations from field measurements: a review. Atmos. Environ. 77, 78–97.

R Core Team, 2013. R: A Language and Environment for Statistical Computing.

Sharma, S., Zhang, M., Anshika, Gao, J., Zhang, H., Kota, S.H., 2020. Effect of restricted emissions during COVID-19 on air quality in India. Sci. Total Environ. 728, 138878.

Shi, X., Brasseur, G.P., 2020. The response in air quality to the reduction of Chinese economic activities during the COVID-19 outbreak. Geophys. Res. Lett. 47, e2020GL088070.

Statheropoulos, M., Vassiliadis, N., Pappa, A., 1998. Principal component and canonical correlation analysis for examining air pollution and meteorological data. Atmos. Environ. 32, 1087–1095.

Vu, T.V., Delgado-Saborit, J.M., Harrison, R.M., 2015. Review: particle number size distributions from seven major sources and implications for source apportionment studies. Atmos. Environ. 122, 114–132.

Washington State Department of Ecology, 2018. Washington State 2014 comprehensive emissions inventory. URL. https://ecology.wa.gov/DOE/files/0d/0dfbc0d0-8485-4620-981b-d6636e1157ee.pdf. (Accessed 17 July 2020).

Washington State Department of Ecology, 2020. Washington air quality advisory. URL. https://fortress.wa.gov/ecy/enviwa/. (Accessed 20 May 2020).

Washington State Department of Transportation, 2020a. Cabinet data sources. URL. https://tracflow.wsdot.wa.gov/loopdata/loop_data_map/. (Accessed 20 May 2020).

Washington State Department of Transportation, 2020b. What's going on with Seattle area traffic with COVID-19?. URL. https://wsdotblog.blogspot.com/2020/03/seattle-area-traffic-covid-19.html. (Accessed 20 May 2020).

Wu, C.-f., Larson, T.V., Wu, S.-y., Williamson, J., Westberg, H.H., Liu, L.-J.S., 2007. Source apportionment of PM2.5 and selected hazardous air pollutants in Seattle. Sci. Total Environ. 386, 42–52.

Xu, K.J., Cui, K.P., Young, L.H., Hsieh, Y.K., Wang, Y.F., Zhang, J.J., et al., 2020. Impact of the COVID-19 event on air quality in central China. Aerosol Air Qual. Res. 20, 915–929.

Yerramshetty, J.S., Akkus, O., 2008. The associations between mineral crystallinity and the mechanical properties of human cortical bone. Bone 42, 476–482.

Zhao, Y.B., Zhang, K., Xu, X.T., Shen, H.Z., Zhu, X., Zhang, Y.X., et al., 2020. Substantial changes in nitrogen dioxide and ozone after excluding meteorological impacts during the COVID-19 outbreak in mainland China. Environ. Sci. Technol. Lett. 7, 402–408.

Zheng, X., Wu, Y., Jiang, J., Zhang, S., Liu, H., Song, S., et al., 2015. Characteristics of on-road diesel vehicles: black carbon emissions in Chinese cities based on portable emissions measurement. Environ. Sci. Technol. 49, 13492–13500.